Available online at www.sciencedirect.com
SCIENCE DIRECT
Journal of Catalysis 240 (2006) 258–267
JOURNAL OF CATALYSIS
www.elsevier.com/locate/jcat

Effect of molybdenum and tungsten on Co/MSU as hydrogenation catalysts

A. Infantes-Molina [a], J. Mérida-Robles [a], E. Rodríguez-Castellón [a], J.L.G. Fierro [b], A. Jiménez-López [a,*]

[a] *Departamento de Química Inorgánica, Cristalografía y Mineralogía (Unidad Asociada al ICP-CSIC), Facultad de Ciencias, Universidad de Málaga, Campus de Teatinos, 29071 Málaga, Spain*

[b] *Instituto de Catálisis y Petroleoquímica, CSIC, Cantoblanco, 28049 Madrid, Spain*

Received 13 December 2005; revised 21 March 2006; accepted 22 March 2006

Abstract

A zirconium-doped mesoporous silica (MSU) was used as a support for Co, CoMo, and CoW catalysts with varying Mo and W loadings. Their activity was tested in the hydrogenation and hydrogenolysis/hydrocracking of tetralin under varying temperatures, experimental conditions, and concentrations of dibenzothiophene (DBT) in a high-pressure, fixed-bed, continuous-flow stainless steel catalytic reactor operating at a pressure of 6.0 MPa. Textural, structural, and metallic properties were studied by XRD, XPS, H_2-TPR, NH_3-TPD, and N_2 adsorption–desorption isotherms. The results indicate that the addition of a promoter, such as W and Mo, improves their catalytic properties in hydrogenation reactions with or without DBT in the feed compared with catalysts containing only cobalt as an active phase. The hydrogenation yield is higher in the case of molybdenum- and tungsten-promoted catalysts, but the molybdenum-promoted catalysts enhances the yield most significantly; with a catalyst containing 5 wt% of Mo at 315 °C with a contact time of 3.6 s and an H_2:tetralin molar ratio of 15, the hydrogenation yield is 93.5%, whereas a catalyst containing 15 wt% of Co gives a yield of 74.0%. The yield of hydrogenolysis/hydrocracking is lower for the promoted catalysts, although those containing tungsten exhibit an intermediate behavior between those containing only cobalt or cobalt and molybdenum as active phases. However, catalysts with molybdenum as a promoter agent have very good thiotolerant properties. With 15 wt% of cobalt and 5 wt% of molybdenum, when 850 ppm of DBT is added to the feed, the conversion of tetralin is nearly 52.0% with a 44.0% yield of hydrogenation products after 6 h on stream; for a catalyst with 15% of cobalt, these values are only 13.1 and 0.9%, respectively, after 5 h on stream.

Keywords: Mesoporous MSU; Cobalt catalysts; Tetralin hydrogenation; Hydrogenolysis/hydrocracking; Sulphur tolerance; Molybdenum; Tungsten

1. Introduction

Research and development of ultra-clean fuel by desulphurization and dearomatization is the goal of numerous researchers in environmental catalysis studies worldwide. Diesel emissions produce a complex mixture of organic and inorganic compounds in the form of gases or small particles that cause more pollution than those generated by gasoline motors. However, diesel engines are preferable over gasoline engines in terms of economy and longevity, and their use is increasing rapidly; hence the search for a breakthrough in the reduction of pollutant emissions to achieve acceptable levels in accordance with established environmental regulations is becoming increasingly important. The aromatics in diesel fuel not only produce undesired emissions in the exhaust gases, but also decrease the cetane number. This has led to new, tighter regulations concerning fuel quality and exhaust emissions and has resulted in the hydrogenation of aromatics as an essential step in the oil-refining process, aimed at producing environmentally friendly fuels. Currently, efforts are being undertaken in this area not only to ameliorate the sulphur content (the amount of sulphur allowed in diesel fuels must be reduced to 1.3×10^{-2} g dL^{-3} by the year 2010 [1], mandating a 97% reduction from current levels), but also to reduce the aromatic content, increase the cetane number [2] to fulfill the specifications of motor fuels [3–5], and decrease the extent of particulate emissions in diesel exhaust gases [4].

* Corresponding author. Fax: +34 952137534.
E-mail address: ajimenezl@uma.es (A. Jiménez-López).

0021-9517/$ – see front matter
doi:10.1016/j.jcat.2006.03.013

Traditionally, the most widely used catalysts in hydrotreating units have been those containing sulphided mixed oxides (NiMo, NiW, and CoMo), even though these can only reach moderate aromatic saturation under typical hydrotreating conditions in a single-stage operation [6] despite their tolerance to sulphur in the feed [7]. To overcome this problem, the industrial approach uses a two-stage process involving a hydrotreating catalyst in the first reactor (i.e., a sulphide catalyst to reduce the sulphur percentage) and a noble metal-containing catalyst in the second reactor that acts on aromatic saturation, with the main drawback being their poisoning when exposed to small quantities of organic sulphur- and nitrogen-containing compounds present in the feed [8,9].

However, it should be pointed out that recently Pd, Pt, and mainly bimetallic Pd–Pt catalysts on several supports have demonstrated relatively high thiotolerance [10–17]. Moreover, the sulphur resistance of a noble metal catalyst is improved by the use of an acidic support [11,18–20], arising from the formation of electron-deficient metal particles interacting with Brönsted acid sites [21] that form a weak bond with sulphur compounds along with the addition of a nonnoble transition metal. Furthermore, Hu et al. [22] have reported improved thiotolerance of Pd catalysts from the addition of a second transition metal, which changed the conversion of toluene from 35.5 to 70.2% over Pd and PdCr, respectively, when 3000 ppm of sulphur was in the feed. This second metal could inhibit the migration of the noble metal to form higher particles due to a decrease in the metal–support interaction after adsorption of H_2S.

The cost of these catalysts due to the expense of the noble metals involved, together with their uncertain thiotolerance, has prompted research into new catalytic systems. Thus, other metals (e.g., Ni, NiW, and PdNi) have been used as active phases in reactions involving the hydrogenation and hydrogenolysis/hydrocracking of aromatic molecules [23–25]. These catalysts are able to catalyse the hydrogenation and ring opening of naphthalenes in the presence of sulphur compounds but usually require extreme operating conditions, such as high hydrogen pressures and temperatures.

The current direction for new research in this area is very diverse. The election of the best active species has been the target of much work, but considering only the active species as the key factor in the preparation of an effective catalyst would be meaningless given that the support participates fully in the catalytic process. It is well known that acidity, pore size, and specific surface area have a pronounced influence on the catalytic results. Such supports as alumina, silica, titania, zeolites, MCM-41, and others have been exhaustively studied [26–28] and shown to participate fully in the catalytic process.

Recently we prepared a series of cobalt catalysts supported on Zr-MSU. This Zr-MSU material was prepared using a nonionic surfactant, polyethyleneoxide, as a template. These surfactants are biodegradable and cheaper than ionic surfactants and thus are promising template agents for the synthesis of new porous materials. The Zr-MSU materials have proven to be stable at high temperatures and to have good stability in aqueous media, mechanical resistance, and under steaming conditions. Their high BET surface areas and high acidity make them excellent candidates for use in heterogeneous catalysis as both acid catalysts and supports. The cobalt-supported catalysts were tested in the hydrogenation, hydrogenolysis, and hydrocracking of tetralin at 6.0 MPa with and without DBT in the feed [29]. They were shown to have good properties in hydrogenation reactions, but after feeding several amounts of DBT, they experience severe deactivation with time. Hence, the main objective is to obtain a hydrogenation cobalt-containing catalyst capable of reducing the quantity of aromatics, but also resisting the sulphur-induced deactivation resulting from the first stage.

The addition of a promoter to these cobalt catalysts could improve their sulphur tolerance, as has been previously demonstrated for noble metal catalysts [30]. In the current work, we have studied the role of tungsten and molybdenum incorporated into Zr-MSU-supported cobalt catalysts in the hydrogenation of tetralin. More to the point, we have attempted to improve both the hydrogenation and thiotolerance of this family of catalysts subjected to predetermined amounts of DBT in the feed.

Bimetallic catalysts with molybdenum have been extensively studied in the HDS reaction. These are indeed most frequently used as first-stage catalysts, but tungsten has been shown to have lower activity than Mo phases [31].

2. Experimental

2.1. Preparation of catalysts

The MSU SiZr7 (Zr-MSU) support was prepared as described elsewhere [32]. For catalyst preparation, the support was pelletized (0.85–1.00 mm) before being impregnated with aqueous solutions of precursor salts via the incipient wetness method; that is, after the first impregnation with a solution of $Co(NO_3)_2{\cdot}6H_2O$, the material was dried at 60 °C (12 h) at atmospheric pressure before the second impregnation with a solution of either $(NH_4)_6Mo_7O_{24}{\cdot}4H_2O$ or a solution of $(NH_4)_6W_{12}O_{39}{\cdot}xH_2O$. After drying in air at 60 °C (12 h) at atmospheric pressure, the samples were calcined at 550 °C for 6 h.

The catalysts were prepared at different cobalt, tungsten, and molybdenum loadings: 10 and 15 wt% for cobalt; 2.5, 5, and 7.5 wt% for molybdenum; and 5 and 13 wt% for tungsten (i.e., the same number of tungsten atoms in a catalyst as molybdenum in the catalysts containing 2.5 and 7.5 wt% of molybdenum). The samples are denoted as CoxMoy and CoxWz, where x, y, and z represent the wt% of cobalt, molybdenum, and tungsten, respectively.

2.2. Characterization of catalysts

Powder X-ray diffraction patterns were obtained using a Siemens D5000 diffractometer (Cu-K_α source) provided with a graphite monochromator. The textural parameters were evaluated from the nitrogen adsorption–desorption isotherms at −196 °C as determined by an automatic ASAP 2020 system from Micromeritics. Elemental chemical analysis was performed with a LECO CHNS 932 analyser.

Hydrogen temperature-programmed reduction (H_2-TPR) experiments were carried out at 50–800 °C using a flow of 10% H_2/Ar (48 ml min^{-1}) and a heating rate of 10 °C min^{-1}. Water produced in the reduction reaction was eliminated by passing the gas flow through a cold finger (−80 °C). The H_2 consumption was controlled by an on-line gas chromatograph (Shimadzu GC-14A) equipped with a thermal conductivity detector (TCD).

Temperature-programmed desorption of ammonia (NH_3-TPD) was carried out to evaluate the total acidity of the catalysts. Catalysts were reduced, at atmospheric pressure, by flowing hydrogen (60 ml min^{-1}) from room temperature to 500 °C at a heating rate of 10 °C min^{-1}, and the sample was maintained at 500 °C for 60 min. After cleaning with helium and adsorption of ammonia at 100 °C, NH_3-TPD was performed at 100–550 °C at a rate of 10 °C min^{-1} using a helium flow. The evolved ammonia was analysed by an on-line gas chromatograph (Shimadzu GC-14A) equipped with a TCD.

X-ray photoelectron spectra were collected using a Physical Electronics PHI 5700 spectrometer with nonmonochromatic Al-K_α radiation (300 W, 15 kV, 1486.6 eV) and a multichannel detector. Spectra of pelletized samples were recorded in the constant pass energy mode at 29.35 eV, using a 720-μm-diameter analysis area. Charge referencing was measured against adventitious carbon (C 1*s* at 284.8 eV). A PHI ACCESS ESCA-V6.0 F software package was used for acquisition and data analysis. A Shirley-type background was subtracted from the signals. All recorded spectra were fitted using Gaussian–Lorentzian curves in to more accurately determine the binding energy of the different element core levels. Because the W 4*f* signal partially overlaps the Zr 4*p* signal from the support, when analysing the W 4*f* signal of W-containing catalysts, the contribution due to the Zr 4*p* signal of the support was considered.

2.3. Catalytic test

The hydrogenation and hydrogenolysis/hydrocracking of tetralin was performed in a high-pressure, fixed-bed, continuous-flow stainless steel catalytic reactor (9.1 mm i.d., 230 mm long) operating at 6.0 MPa of pressure (4.5 MPa H_2 and 1.5 MPa N_2). Before the activity test, 3 cm^3 of catalyst (particle size 0.85–1.00 mm) was reduced at atmospheric pressure by flowing hydrogen (60 ml min^{-1}) from room temperature to 500 °C at a rate of 10 °C min^{-1}. The sample was maintained at 500 °C for 60 min, after which the N_2 and H_2 gases were mixed with a solution of tetralin (THN) in *n*-heptane (10 vol%) supplied by a Gilson 307SC piston pump (model 10SC) (with a liquid hourly space velocity [LHSV] of 4.0–9.0 h^{-1}), then introduced into the reactor. The thiotolerance of the catalysts was evaluated by adding two different concentrations of DBT in the feed (425 and 850 ppm wt for normal and severe sulphur poisoning tests, respectively). The reactant and products were studied by collecting liquid samples after 1 h on stream once the temperature had increased to the desired value (for study of the effect of temperature) or after each hour (for study of the effect of time). These samples were then analysed by gas chromatography (Shimadzu GC-14B, equipped with a FID and a TRB-1 capillary column, coupled to a Shimadzu AOC-20i automatic injector). After the majority were identified, they were classified into the following groups: (i) volatile compounds (VC), including noncondensable C_1–C_6 products calculated from the carbon balance of the reaction; (ii) hydrogenation products, including *trans*- and *cis*-decalin (HYD); (iii) hydrocracking and hydroisomerisation compounds (HHC), including alkylbenzenes and polyalkylolefins; and (iv) naphthalene. No products heavier than decalins were found. Note that high yields of hydrogenation products, especially cracking compounds, gave rise to an increase in the cetane number of fuels.

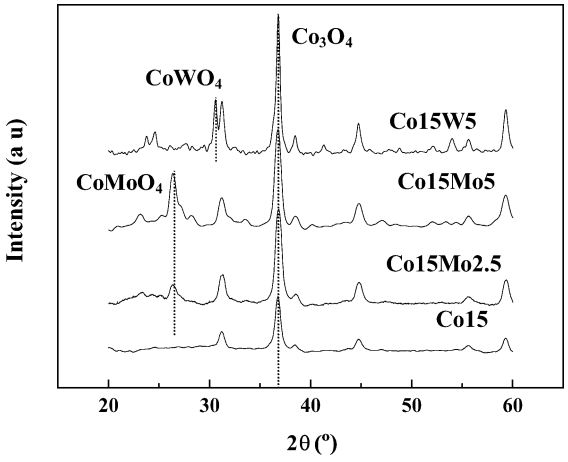

Fig. 1. X-Ray diffractograms of the calcined catalysts.

3. Results and discussion

The catalysts were characterized to gain more insight into the results. The activity and yield depend on the metal and acid sites, because the balance between them affects the performance in hydrocracking and hydroisomerisation.

X-ray diffractograms of the calcined samples are given in Fig. 1. All of the catalysts show the characteristic diffraction lines of Co_3O_4. The diffractograms of catalysts containing molybdenum show peaks corresponding to $CoMoO_4$, with the intensities of these peaks increasing with increasing amounts of molybdenum in the catalyst. Similarly, the diffractogram of the catalyst containing tungsten exhibits a reflection line at $2\theta = 30.6°$, corresponding to a $CoWO_4$ phase plus the reflection lines of Co_3O_4. These results agree well with those reported in the literature, where such phases are formed on heating at similar calcination temperatures [33,34].

After the samples are reduced with hydrogen at 500 °C, reflection lines of spinel type structures do not appear, and only the reflection lines attributed to metallic cobalt are observed. Given the H_2-TPR curves, the complete reduction of the ionic species cannot be assumed. There are oxidized species that can be reduced only at temperatures above 500 °C. These metallic oxides must form compounds with lower-oxidation states and, as detected by XRD, are well dispersed. Zhang et al. [35], in a study of the reducibility of samples containing cobalt and tungsten in different compositions, found that samples with high

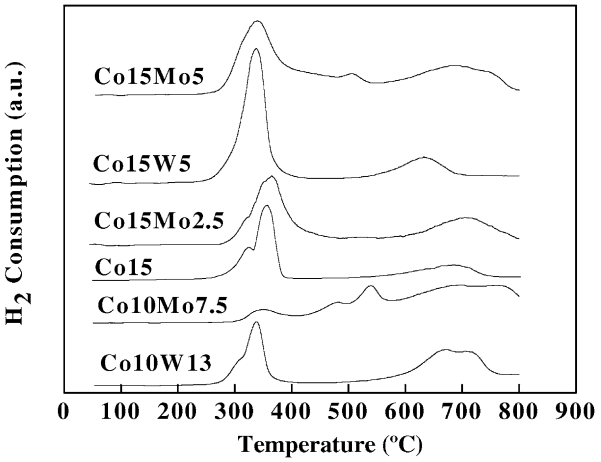

Fig. 2. H_2-TPR profiles of Co, CoMo, CoW catalysts.

cobalt content were more easily reduced and that the phases present in the reduced samples also varied with the cobalt content. The formation of Co_3W and W could be detected in samples containing high cobalt loadings at a reduction temperature of 600 °C. In our case, these phases were not detected by XRD, probably due to their low content and high dispersion, if indeed they were present at all.

To determine the type and reducibility of the Co and Mo species present in the catalytic precursors, H_2-TPR experiments were carried out on the oxidizes precursor samples. Fig. 2 shows the H_2-TPR patterns of this series of solids. When Mo is added to the catalysts, the H_2-TPR profiles are modified with regard to that of the Co15 catalyst. Thus, Co10Mo7.5 exhibits a small H_2 consumption peak at 350 °C corresponding to the reduction of Co_3O_4 to Co^0 [29], and new reduction peaks appear at 480 and 540 °C, indicating the reduction of cobalt and part of the molybdenum-forming part of the $CoMoO_4$ spinel. Finally, close to 700 °C, a broad and ill-defined band appears in all cases, assigned to the reduction of the Co^{2+} as Co_2SiO_4. This compound is formed during the calcination of samples at 550 °C (for 6 h) after the impregnation process. The shoulder at close to 800 °C could correspond to the reduction of Mo(VI) to Mo(IV), because it does not appear in the Co15 H_2-TPR profile. In the case of Co15Mo*y* catalysts, note that the main reduction peak shows a tail at higher temperatures, which can be ascribed to the reduction of Co^{2+}-forming $CoMoO_4$, as well as a small peak at 510 °C due to the reduction of Mo(VI) to Mo(IV) forming such a spinel.

Meanwhile, in the case of catalysts containing tungsten, two main reduction peaks appear for the Co15W5 catalysts, one centred at 340 °C and the other centred at 635 °C. Comparing the relative intensity of the peak at 340 °C with that of Co15 at the same temperature clearly shows the higher intensity of the former. This peak may correspond not only to the reduction of the cobalt species, but also to the partial reduction of Co^{2+}*y*W(VI)-forming $CoWO_4$. The peak at high temperatures shifts to lower temperatures compared to the Co15 catalyst. This could correspond to the reduction of cobalt-forming cobalt silicate. But when tungsten is at higher loading, as on Co10W13, a new shoulder at 730 °C is observed that can be assigned to the reduction of W(VI) to W(IV). Comparing the H_2-TPR profile of Co15Mo2.5 with its tungsten counterpart (i.e., Co15W5) clearly shows that tungsten improves the reducibility of the cobalt species; hence cobalt reduction is more difficult for Co15Mo2.5, and, consequently, an important fraction of cobalt remains unreduced. This fact could explain the high surface acidity found for this catalyst.

Having studied the H_2-TPR curves, we chose a reduction temperature of 500 °C. At this temperature, the main peak disappears, and the possible agglomeration of active phases at higher temperatures is avoided.

The textural characteristics—specific surface area (S_{BET}), total pore volume (V_p), and mean pore diameter—are given in Table 1. These were determined from nitrogen adsorption isotherms measured at −196 °C. The lowest S_{BET} values are for doped catalysts containing 10 wt% of cobalt, where a reduction in the pore volume is also found. Importantly, the Co10Mo7.5 catalyst has the lowest pore volume and the highest mean pore diameter. This fact can be explained by taking into account the pore size distribution, in which two overlapped maxima are detected, one at 17.0 Å (due to the support) and the other at 22.5 Å, possibly due to deposition of molybdenum–cobalt mixed oxides, which have their own specific surface area [36]. This effect is greatly reduced for catalysts containing 15 wt% of cobalt, however, possibly because cobalt oxide itself forms this structure at cobalt loading of 15 wt%. Addition of molybdenum or tungsten leads to formation of new particles of mixed oxides, which block the access to mesopores; thus the specific surface area is not significantly reduced.

As determined by NH_3-TPD, incorporation of cobalt, molybdenum, and tungsten leads to a decrease in specific surface acidity. Table 2 gives the total acidity and the values corre-

Table 1
Textural properties of the support and the calcined materials

Sample	S_{BET} ($m^2\ g^{-1}$)	V_p ($cm^3\ g^{-1}$)	d_p (av) (Å)
ZrMSU	493	0.25	18.6
Co10	361	0.18	19.0
Co10W13	285	0.15	19.8
Co10Mo7.5	146	0.09	22.9
Co15	338	0.17	19.5
Co15W5	306	0.17	18.8
Co15Mo2.5	309	0.17	20.0
Co15Mo5	313	0.17	20.6

Table 2
Quantity of ammonia desorbed at different intervals of temperature for reduced catalysts

	mmol $NH_3\ g^{-1}$						
T (°C)	100–200	200–300	300–400	400–500	500–550	550 Isot	Total
Co10	82.2	270.5	155.9	61.0	12.5	23.0	605.0
Co10Mo7.5	95.9	160.9	91.5	65.4	20.7	25.4	459.8
Co10W13	125.0	195.0	75.7	43.4	25.2	81.4	545.7
Co15	55.9	258.1	191.8	98.0	31.8	61.9	697.7
Co15Mo2.5	164.0	250.5	203.2	101.1	20.4	22.7	761.9
Co15W5	127.1	214.0	73.1	5.3	1.0	2.4	422.9
Co15Mo5	155.8	200.0	102.0	46.5	11.5	12.3	528.1

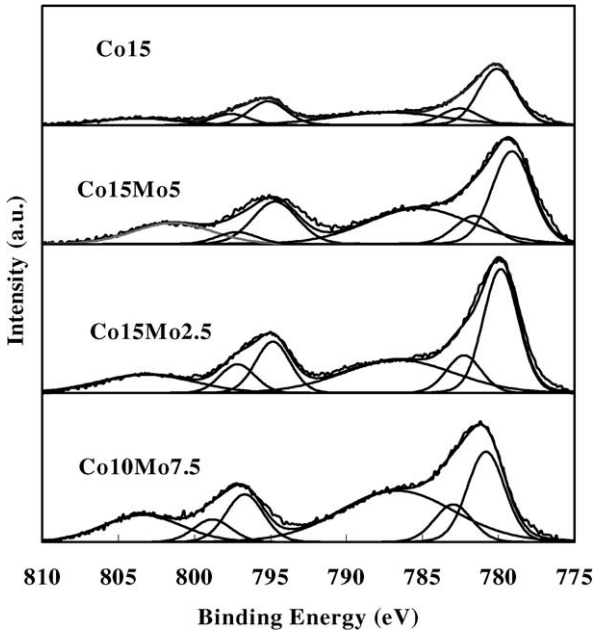

Fig. 3. Co $2p$ photoelectron spectra of calcined CoxMoy catalysts.

sponding to different temperature intervals. All of the doped catalysts except Co15Mo2.5 show lower superficial acidity than their cobalt pristine counterparts. As Mo or W are added in a second step on cobalt salt, a superficial layer of $CoMoO_4$ spinel is formed that is responsible for the decrease in total acidity. This is due not only to the weak tendency of these species to retain ammonia molecules, but also to the partial blockage of pores, as was seen in the surface area values.

X-Ray photoelectron spectra of both calcined and reduced Cox, CoxMoy, and CoxWz catalysts are useful for determining the chemical state of the different elements. The Si $2p$ and Zr $2p$ core-level spectra of calcined and reduced samples are similar and show binding energies of about 103.3 and 183.2 eV, respectively. Table 3 gives the corresponding binding energies of Co $2p_{3/2}$, Mo $3d_{5/2}$, and W $4f_{7/2}$. The Co $2p$ spectra of calcined CoxMoy catalysts (Fig. 3) are characterized by a main peak centred at about 780.0 eV and another small peak at 782.4 eV. Although the first peak is difficult to assign because it can correspond to Co^{3+} and/or Co^{2+} (with this Co^{2+} coming from Co_3O_4 and $CoMoO_4$ for molybdenum-containing samples), the small peak at a higher binding energy is due to Co^{2+} from Co_2SiO_4, because the reduction of this cobalt species is difficult. In the case of calcined samples, the observed differences in the binding energies of the Co $2p_{3/2}$ main peak are between 0.1 and 0.9 eV. However, these differences are greater for reduced samples, likely due to the different sizes of cobalt species after the addition of Mo or W. A very broad shakeup satellite peak at 6 eV from the main Co $2p_{3/2}$ can be seen. The intensity of this satellite is much stronger in Mo-doped catalysts than in Co10 and Co15 ones, indicating that reduction of the Co^{2+}-forming part of $CoMoO_4$ is more difficult than that of Co_3O_4 [37].

The relative intensity of these satellite peaks was used to identify the cobalt species; the higher their intensity, the greater the amount of $CoMoO_4$ formed. This fact is confirmed in Fig. 3,

Table 3
Spectral parameters obtained by XPS analysis

Sample	BE (eV) Co $2p_{3/2}$		BE (eV) Mo $3d_{5/2}$ y W $4f_{7/2}$	
	Calcined	Reduced	Calcined	Reduced
Co_2SiO_4	781.9	–	–	–
Co_3O_4	779.5	–	–	–
Co10		778.7 (38%)		
	780.2 (76%)	780.8 (44%)		
	782.4 (24%)	782.9 (18%)		
Co10Mo7.5		777.8 (49%)		
	780.8 (70%)	780.2 (36%)		228.2 (61%)
	782.9 (30%)	782.5 (15%)	231.8	231.0 (29%)
Co10W13		777.7 (32%)		
	779.9 (79%)	779.7 (47%)		32.1 (23%)
	782.1 (21%)	781.7 (21%)	35.3	35.2 (77%)
Co15		778.8 (38%)	–	–
	780.0 (77%)	780.8 (44%)		
	782.5 (23%)	782.7 (18%)		
Co15Mo2.5		777.7 (38%)		
	779.8 (76%)	779.9 (38%)		229.3 (48%)
	782.2 (24%)	781.6 (24%)	232.2	231.9 (52%)
Co15W5		777.4 (38%)		
	779.6 (78%)	779.7 (39%)		32.4 (43%)
	782.1 (22%)	781.6 (23%)	35.2	35.3 (57%)
Co15Mo5		777.7 (33%)		
	779.1 (77%)	779.5 (51%)		228.4 (50%)
	781.6 (23%)	781.5 (16%)	231.7 (100%)	231.1 (50%)

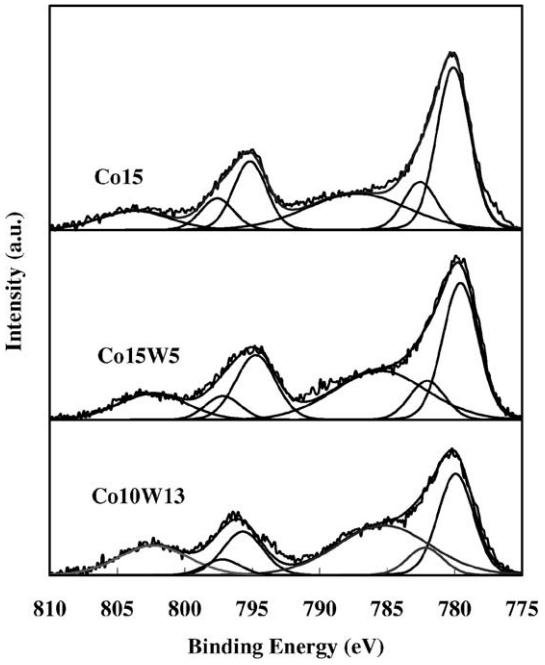

Fig. 4. Co $2p$ photoelectron spectra of calcined CoxWz catalysts.

where samples with molybdenum suffer an increase in the intensity of the shakeup satellite peak. The same results can be seen in the spectra of the calcined catalysts containing tungsten (Fig. 4).

Fig. 5 shows the Mo 3*d* core-level spectra of the Co15Mo5 catalyst when calcined, reduced, and used with 850 ppm of DBT in the feed. Before reduction, the doublet Mo $3d_{5/2}$ and Mo $3d_{3/2}$ appears at 231.8 and 234.9 eV, which is characteristic of the Mo(VI) species [38–40]. The Mo 3*d* core-level spectrum after reduction shows, besides this doublet, a new one at 228.2 and 231.3 eV that is characteristic of Mo(IV) [38], indicating that a partial reduction of Mo(VI) occurs under these experimental conditions.

With regard to the samples containing tungsten as a promoter, Fig. 6 shows that the W $4f_{7/2}$ signal gives a peak close to 35.2 eV that corresponds to $CoWO_4$, as previously detected by XRD. The weak peak at 30.6 eV corresponds to interference of the Zr $4p$ signal by Zr(IV) in the support. After the reduction process, a new peak at 32.4 eV appears that is assigned to W(IV) [41].

Catalysts with different compositions were tested to study the role of molybdenum and tungsten on cobalt catalysts in aromatic hydrogenation reactions. The activity of these catalysts was evaluated by considering both the degree of conversion of tetralin and the yield of hydrogenation products, because the latter is of particular interest for reducing diesel pollutant emissions.

A first reference catalyst containing 10 wt% of cobalt, Co10, was selected, taking previous results into account [29]. With the aim of augmenting catalytic performance, two promoters (7.5 wt% of molybdenum or 13 wt% of tungsten) were added to this catalyst, giving rise to Co10Mo7.5 and Co10W13 catalysts, respectively. The activity of these catalysts was tested in the temperature range of 275–375 °C. Fig. 7 shows the tetralin conversions for the Co10, Co10Mo7.5, and Co10W13 catalysts. Clearly, molybdenum and tungsten do not improve the catalytic

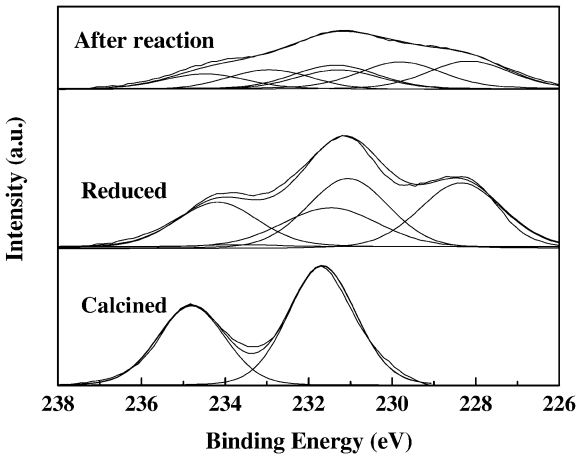

Fig. 5. Mo 3*d* photoelectron spectra of Co15Mo5 catalyst.

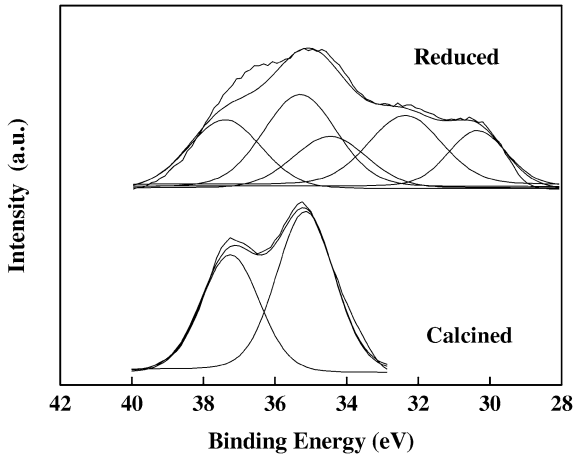

Fig. 6. W $4f_{7/2}$ core level signal for Co15W5 catalyst.

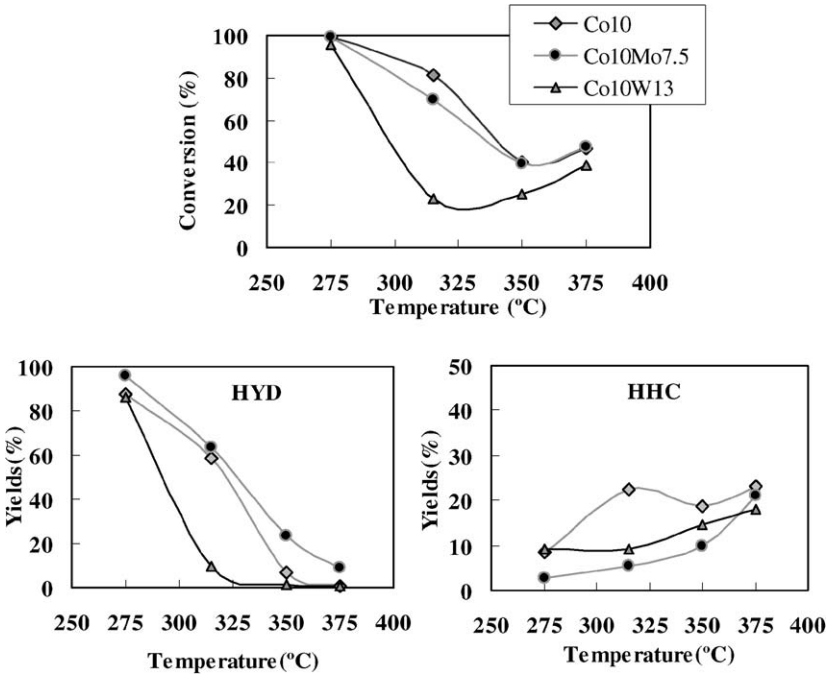

Fig. 7. Plot of conversion and yields versus temperature for hydrogenation of tetralin. Experimental conditions: H_2/THN molar ratio = 10, pH_2 = 4.5 MPa, pN_2 = 1.5 MPa, LHSV = 6 h^{-1}, GHSV = 1300 h^{-1}, contact time = 2.8 s.

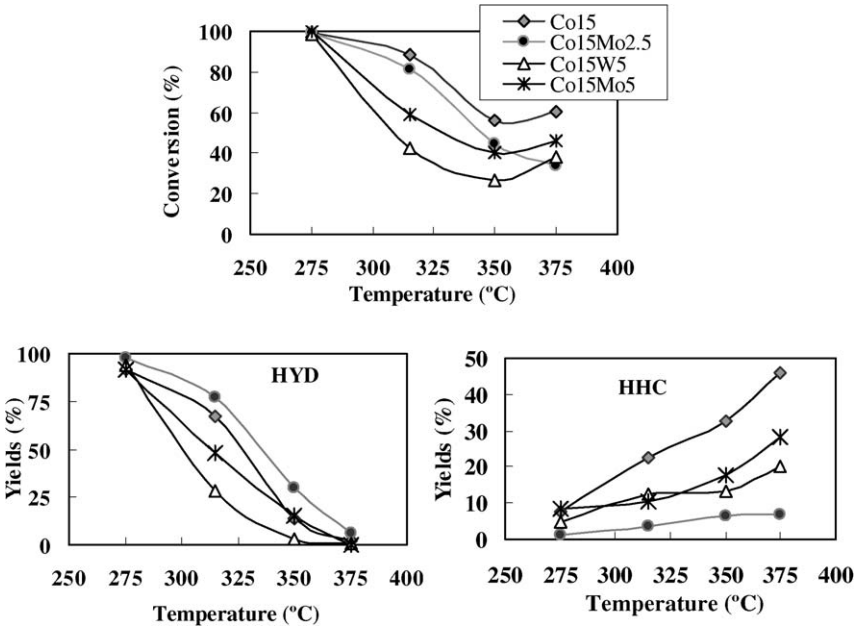

Fig. 8. Plot of conversion and yields versus temperature for hydrogenation of tetralin. Experimental conditions: H_2/THN molar ratio = 10, pH_2 = 4.5 MPa, pN_2 = 1.5 MPa, LHSV = 6 h^{-1}, GHSV = 1300 h^{-1}, contact time = 2.8 s.

behavior of the cobalt catalyst under these conditions. Co10 and Co10Mo7.5 exhibit almost the same conversion patterns and yields of hydrogenation products; however, the highest yield of HHC is still given by Co10. The Co10W13 catalyst exhibits a much lower conversion and yield of HYD but a better yield of HHC than Co10Mo7.5. The higher reducibility of this catalyst, which could contain a layer of reduced W(IV) over the metallic cobalt, may be responsible for this behavior, because this layer can hinder the access of H_2 to the metallic Co^0 particles, thereby reducing its catalytic activity. Clearly, cobalt plays a key role in the catalytic performance of these materials.

Taking these results into account, and considering only the Co10 and Co10Mo7.5 catalysts, a test using a feed with 425 ppm of DBT was carried out at 315 °C. With Co10, the conversion changed from 81.1 to 9.5% after 6 h on stream, whereas with Co10Mo7.5, conversion changed from 69.6 to 23.6% in the same period. This finding demonstrates the important role of molybdenum with the presence of DBT in the feed.

To optimize its performance, several changes in the experimental conditions were made for Co10Mo7.5 in the absence of DBT. A conversion of 91.5% was attained under the new experimental conditions (i.e., an H_2/THN molar ratio of 10 and 3.6 s of contact time), while maintaining a reaction temperature of 315 °C. Under these same conditions, a new study of thiotolerance was carried out for the Co10Mo7.5 catalyst using 425 ppm of DBT in the feed. Again, after 6 h on stream, partial deactivation occurs, changing the conversion from 91.5 to 41.5%, the yield of HYD from 80.1 to 34.1%, and the yield of HHC from 11.2 to 4.2%. So far, although no improvement in conversion was achieved for the Co10 catalyst, it would seem that adding Mo leads to improved resistance to feeds containing sulphur compounds, such as DBT.

The observed improvement in thiotolerance but no improvement in activity prompted us to test a new series of catalysts with 15 wt% of cobalt, 2.5 and 5 wt% of molybdenum, and 5 wt% of tungsten (i.e., equivalent to its counterpart of Mo 2.5 wt%). The results of this testing are shown in Fig. 8. Although Co15 displays the best conversion pattern, Co15Mo2.5 shows the highest yields of hydrogenation products. It is possible that the presence of a small amount of molybdenum(IV) induces better Co^0 dispersion. Simultaneously, Mo(IV) can act as an acid center in which tetralin molecules are retained and hydrogenated by H_2 spillover from the metallic particles.

Bearing this in mind, molybdenum-containing catalysts give a lower HHC yield compared with catalysts based on cobalt because the former have fewer acid centres, which are responsible for the formation of HHC. Considering total acidity, Co15Mo2.5 desorbs the most ammonia molecules but has the lowest HHC yield. This could be due to the existence of more Co^{2+} ions capable of forming amino complexes, which creates a high specific surface acidity. These ions are not strong enough to produce HHC, however. In fact, observing the values of ammonia desorbed at different temperatures, Co15Mo2.5, Co15W5, and Co15Mo5 desorb much more ammonia than Co15 at 100–200 °C. This ammonia could be responsible for formation of the amino complexes and is not indicative of the strong acidity of these materials. In any case, it should be taken into account that metallic cobalt particles in Co15 catalyst can exhibit good activity in tetralin hydrogenolysis reactions, and that after doping with Mo/W, the activity in hydrogenolysis reactions is lower.

New experiments were carried out by changing the experimental conditions to improve the catalytic results at 315 °C (Table 4). In all cases, the conversion increases at higher contact times and hydrogen:tetralin molar ratios. Thus, for a contact time of 3.6 s and an H_2:THN molar ratio of 15, the conversion for all catalysts is close to 100%, and the HYD product yield is greatly increased. The behavior of doped catalysts is similar to

Table 4
Catalytic properties of the supported cobalt, cobalt–molybdenum, cobalt–tungsten catalysts in the hydrogenation, hydrogenolysis/hydrocracking of tetralin at 315 °C

τ (s)[a]	H_2/THN[b]	315 °C	Co15	Co15Mo2.5	Co15W5	Co15Mo5
2.8	10	Conversion	88.7	80.9	42.2	58.8
		Yield				
		HYD	66.9	76.9	21.2	48.1
		HHC	22.4	3.7	11.7	10.6
3.6	10	Conversion	99.2	99.0	98.7	90.4
		Yield				
		HYD	72.1	88.7	77.5	82.6
		HHC	26.1	10.0	17.2	7.7
3.6	15	Conversion	99.0	99.6	98.9	100
		Yield				
		HYD	74.0	86.0	83.0	93.5
		HHC	24.7	13.6	15.8	5.7

[a] Contact time.
[b] Molar ratio.

that of the Co15 catalyst [29]; the longer the contact time and the higher the H_2:THN molar ratio, the better the results. However, increasing conversion and hydrogenation product yield is stressed to a greater degree than for cobalt catalysts. Thus, the main promoting effect of molybdenum is an increase in the hydrogenation capability of these catalytic systems, because all of these catalysts contain superficial Mo(IV) or W(IV), as deduced from XPS studies, not only the total acidity, but also the strength of this acidity of these catalysts is lower than that of Co15. This allows the acid sites to retain tetralin molecules, resulting in their hydrogenation by spillover, although they are not strong enough to produce HHC products. The production of naphthalene and volatile compounds is negligible, if it occurs at all.

To complete the study of the promoting effect of molybdenum and tungsten, 425 ppm of DBT was fed under the most favourable experimental conditions (Fig. 9) and also at 315 °C. With increasing time on stream, DBT sulphur poisons the catalysts, leading to a decrease in catalytic activity. All catalysts, but especially Co15 and Co15W5, show a decrease in total conversion after 6 h in the presence of DBT in the feed. Only for catalysts containing Mo is the yield of HYD products high, being >85.0% after 6 h on stream. Both catalysts produce high yields of HYD products but low percentages of HHC compounds.

Fig. 10 shows the results with 850 ppm of DBT in the feed. The influence becomes more pronounced, and after 4 h on stream Co15 suffers severe deactivation, whereas Co15Mo5 shows a conversion of 52.2% and a yield of hydrogenation products of 44.1% after 6 h on stream. Co15Mo2.5 shows an intermediate behavior, with a conversion of 27.0% and an HYD yield of 23.3% after 6 h on stream. The observed improvement obtained by adding molybdenum to the catalytic system is clear, with increased conversion and HYD yield, the latter of which is of great interest when considering the pollutant effects of aromatic molecules. This may indicate the possible formation of molybdenum sulphide. Elemental chemical analysis of the catalysts show that after working with 425 ppm of DBT in the feed, the amount of sulphur found in the sample was practically zero in all cases, but after working with 850 ppm of DBT in the feed, the presence of sulphur was observed in the catalyst containing molybdenum after the catalytic reaction (Table 5), suggesting the possible formation of molybdenum sulphide. This is well known in hydrotreating units that use CoMo catalysts, in which

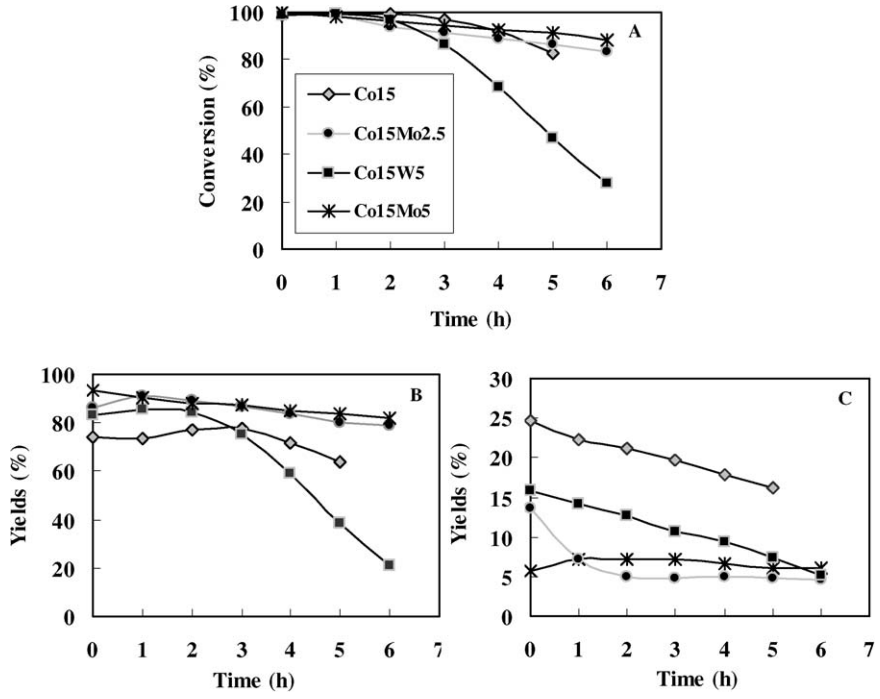

Fig. 9. Variation of the conversion (A), yields of HYD (B) and yields of HHC (C) on time on stream, after feeding 425 ppm of DBT. Experimental conditions: H_2/THN molar ratio = 15, pH_2 = 4.5 MPa, pN_2 = 1.5 MPa, LHSV = 4 h^{-1}, GHSV = 1000 h^{-1}, contact time = 3.6 s.

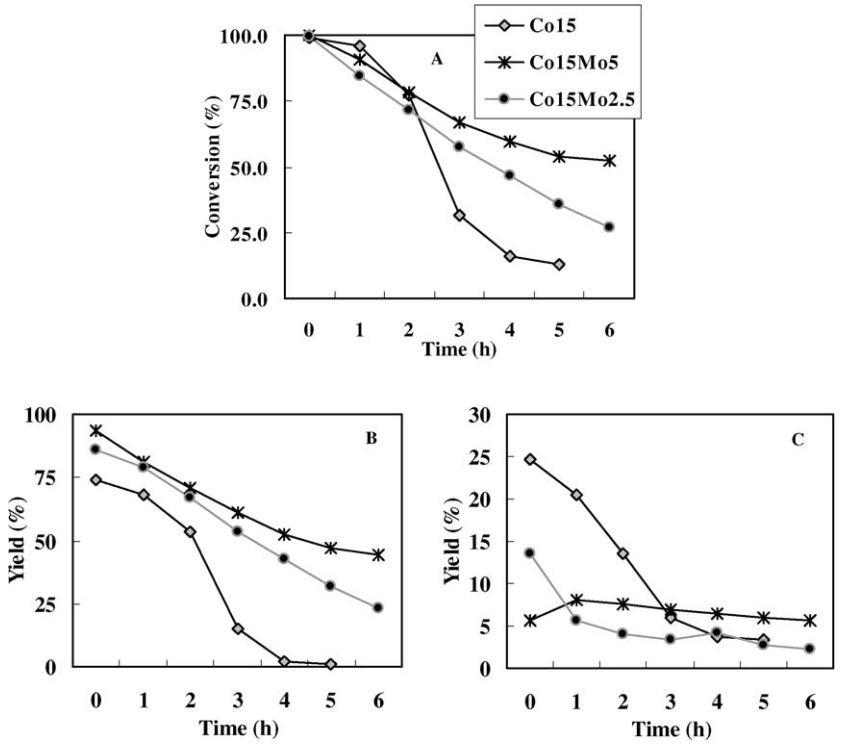

Fig. 10. Variation of the conversion (A), yields of HYD (B) and yields of HHC (C) on time on stream, after feeding 850 ppm of DBT. Experimental conditions: H_2/THN molar ratio = 15, pH_2 = 4.5 MPa, pN_2 = 1.5 MPa, LHSV = 4 h^{-1}, GHSV = 1000 h^{-1}, contact time = 3.6 s.

Table 5
Elemental chemical analysis

	Used[a]		
	%C	%H	%S
Co15	0.595	0.796	0.042
Co15Mo2.5	0.705	1.135	0.077
Co15Mo5	0.736	0.616	0.156

[a] After feeding 850 ppm of DBT.

a good level of hydrogenation activity is found. The amount of sulphur found in the spent Co15Mo5 catalyst is equivalent to 0.1 mol S (mol Mo)$^{-1}$. Thus, in the experimental conditions under which DBT is fed (315 °C), only the formation of a superficial MoS_2 can be expected. In contrast, for Co15, the amount of sulphur is very low (0.005 mol S (mol Co)$^{-1}$) after 850 ppm of DBT is fed; thus, in this case, the formation of CoS_2 can be discarded. In a previous work [29], we have established that Co15 deactivation results from the agglomeration of metal particles caused by the presence of sulphur, as confirmed by chemisorption measurements.

Our results highlight the promoting effect of molybdenum over that of tungsten, possibly due to the greater amount of Mo(IV) on the surface, which is capable of reacting with sulphur to form MoS_2. The results were obtained with XPS, where the Mo 3*d* core-level spectra of used Co15Mo5 catalyst (Fig. 5) were fitted with three Mo 3*d* doublets: the doublets of Mo(VI) and Mo(IV) and an additional one with the main Mo $3d_{5/2}$ peak at 230.0 eV ascribed to the presence of MoS_2 [42]. The formation of molybdenum sulphide can be assumed, although no sulphide was detected by this technique. Therefore, the higher activity of the molybdenum catalysts with DBT in the feed compared with those without can be explained by the formation of MoS_2, which, besides eliminating the sulphur compounds, also maintains a high hydrogenation activity.

All used catalysts were calcined and reduced under the same initial conditions, and then tested again to ensure their regeneration properties. The same patterns of conversion and yields were obtained, indicating that they undergo only reversible deactivation.

4. Conclusion

The activity of Mo- and W-doped cobalt catalysts supported on zirconium-doped mesoporous silica (MSU) with different cobalt, molybdenum, and tungsten loadings was studied in the hydrogenation and hydrogenolysis/hydrocracking of tetralin with and without DBT in the feed and at several experimental conditions, to optimize their performance in this reaction. Our results indicate that the addition of W and Mo improves the catalytic properties of monometallic cobalt catalysts. Thus, operating under the optimum experimental conditions, the hydrogenation yields are higher for catalysts promoted with molybdenum and with tungsten (Table 4), but much higher for those promoted with molybdenum. In this sense, under the optimum experimental conditions, the hydrogenation yield was 93.5% for the Co15Mo5 catalyst and 74.0% for the Co-15 catalyst. However, the yield of hydrogenolysis/hydrocracking is lower for the molybdenum- and tungsten-promoted catalysts, although the tungsten-promoted catalyst exhibits an intermedi-

ate behavior between the cobalt- and molybdenum-promoted ones as active phases.

Related to thiotolerant properties, catalysts promoted with molybdenum (specifically, Co15Mo5) exhibit the best performance. With 425 ppm of DBT in the feed, Co15Mo5 shows a constant conversion of 88.2% after 6 h on stream, with a yield of HYD products close to 82.0% but a low yield of HHC products (7.0%). With 850 ppm of DBT in the feed, the conversion of tetralin is close to 52.0%, and the yield of hydrogenation products after 6 h on stream is 44.0%. For its counterpart with only cobalt (i.e., Co-15), these values are only 13.1 and 0.9%, respectively, after 5 h on stream.

Acknowledgments

The authors gratefully acknowledge the Ministerio de Ciencia y Tecnología (Spain) (project MAT2003-02986) and EU Commission's GROWTH Program (contract G5RD-CT-2001-0537) for funding this work. A.I.M. also thanks the Ministerio de Ciencia y Tecnología (Spain) for a fellowship.

References

[1] Environmental Protection Agency, Federal Register 65 (2000) 35430.
[2] G.H. Unzelman, Oil Gas J. (June 29, 1987).
[3] A. Avidan, B. Klein, R. Ragsdale, Hydrocarbon. Process. 80 (2) (2001) 47.
[4] A. Stanislaus, B.H. Cooper, Catal. Rev. Sci. Eng. 36 (1994) 75.
[5] B. Pawelec, R. Navarro, J.L.G. Fierro, J.F. Cambra, F. Zugazaga, M.B. Güemer, P.L. Arias, Fuel 76 (1) (1997) 61.
[6] H. Cooper, B.B.L. Donnis, Appl. Catal. A 137 (1996) 203.
[7] K. Sato, Y. Iwata, T. Yoneda, A. Nishijima, Y. Miki, H. Shimado, Catal. Today 45 (1998) 367.
[8] C.H. Bartholomew, P.K. Agraval, J.R. Katzer, in: D.D. Eley, H. Pines, P.B. Weisz (Eds.), Advances in Catalysis, vol. 31, Academic Press, New York, 1982, pp. 135–242.
[9] J. Barbier, E. Lamy-Pitara, P. Marecot, J.P. Boitiaux, J. Cosyns, F. Verna, in: D.D. Eley, H. Pines, P.B. Weisz (Eds.), Advances in Catalysis, vol. 37, Academic Press, San Diego, CA, 1990, pp. 279–318.
[10] S. Albertazzi, G. Busca, E. Finocchio, R. Glöckler, A. Vaccari, J. Catal. 223 (2004) 372.
[11] R.M. Navarro, B. Pawelec, J.M. Trejo, R. Mariscal, J.L.G. Fierro, J. Catal. 189 (2000) 184.
[12] A.D. Schmitz, G. Bowers, C. Song, Catal. Today 31 (1996) 45.
[13] M.J. Martinez-Ortiz, G. Fetter, J.M. Domínguez, J.A. Melo-Banda, R. Ramos-Gómez, Microporous Mesoporous Mater. 58 (2003) 73.
[14] S.K. Maity, J. Ancheyta, L. Soberanis, F. Alonso, M.E. Llanos, Appl. Catal. A 244 (2003) 141.
[15] P. Afanasiev, M. Cattenot, C. Geannet, N. Matsubayashi, K. Sato, S. Shimada, Appl. Catal. A 237 (2002) 227.
[16] M. Jacquin, D.J. Jones, J. Roziére, S. Albertazzi, A. Vaccari, M. Lenarda, L. Storaro, R. Ganzerla, Appl. Catal. A 251 (2003) 131.
[17] E. Rodríguez-Castellón, J. Mérida-Robles, L. Díaz, P. Maireles-Torres, D.J. Jones, J. Rozière, A. Jiménez-López, Appl. Catal. A 260 (2004) 9.
[18] A. Corma, A. Martinez, S.V. Martinez, J. Catal. 169 (1997) 480.
[19] H. Yasuda, T. Sato, Y. Yoshimura, Catal. Today 50 (1999) 63.
[20] T. Fujikawa, K. Idei, K. Usui, Sekiyu Gakkaishi 42 (1999) 4.
[21] W.M.H. Sachtler, A.Y. Stakheev, Catal. Today 12 (1992) 283.
[22] L. Hu, G. Xia, L. Qu, C. Li, Q. Xin, D. Li, J. Mol. Catal. A 171 (2001) 169.
[23] E. Rodriguez-Castellón, L. Díaz, P. Braos-García, J. Mérida-Robles, P. Maireles-Torres, A. Jiménez-López, A. Vaccari, Appl. Catal. A 249 (2003) 83.
[24] D. Eliche-Quesada, J. Mérida-Robles, P. Maireles-Torres, E. Rodríguez-Castellón, G. Busca, E. Finocchio, A. Jiménez-López, J. Catal. 220 (2003) 457.
[25] V.L. Barrio, P.L. Arias, J.F. Cambra, M.B. Güemez, B. Pawelec, J.L.G. Fierro, Appl. Catal. A 242 (2003) 17.
[26] T. Chiranjeevi, G. Muthu Kumaran, J.K. Gupta, G. Murali Dhar, Catal. Commun. 6 (2005) 101.
[27] M.A. Arribas, A. Corma, M.J. Díaz-Cabañas, A. Martínez, Appl. Catal. A 273 (2004) 277.
[28] U.R. Pillai, E. Sahle-Demessie, Appl. Catal. A 281 (2005) 331.
[29] A. Infantes-Molina, J. Mérida-Robles, E. Rodríguez-Castellón, B. Pawelec, J.L.G. Fierro, A. Jiménez-López, Appl. Catal. A 286 (2005) 239.
[30] V. Ponec, Appl. Catal. A 222 (2001) 31.
[31] Y. Okamoto, A. Kato, Usman, K. Sato, I. Hiromitsu, T. Kubota, J. Catal. 233 (2005) 16.
[32] A. Infantes-Molina, J. Mérida-Robles, P. Maireles-Torres, E. Finocchio, G. Busca, E. Rodríguez-Castellón, J.L.G. Fierro, A. Jiménez-López, Microporous Mesoporous Mater. 75 (2004) 23.
[33] V. La Parola, G. Deganello, A.M. Venezia, Appl. Catal. A 260 (2004) 237.
[34] M. Ferrari, B. Delmon, P. Grange, Carbon 40 (2002) 497.
[35] Z. Zhang, Y. Zhang, M. Muhammed, Int. J. Refract. Met. Hard Mater. 20 (2002) 227.
[36] F. Dumeignil, K. Sato, M. Imamura, N. Matsubayashi, E. Payen, H. Shimada, Appl. Catal. A 287 (2005) 135.
[37] T.I. Korányi, I. Manninger, Z. Paál, O. Marks, J.R. Gunter, J. Catal. 116 (1989) 422.
[38] H. Shimada, T. Sato, Y. Yoshimura, J. Hiraishi, A. Nishijima, J. Catal. 110 (1988) 275.
[39] L. Portela, P. Grange, B. Delmon, J. Catal. 156 (1995) 254.
[40] A.M. Venezia, V. La Parola, G. Deganello, D. Cauzzi, G. Leonardi, G. Predieri, Appl. Catal. A 229 (2002) 261.
[41] J.F. Moulder, W.F. Stickle, P.E. Sobol, K.D. Bomben, in: J. Chastain (Ed.), Handbook of X-Ray Photoelectron Spectroscopy, Perkin–Elmer, Minneapolis, 1992.
[42] J. Mérida-Robles, E. Rodríguez-Castellón, A. Jiménez-López, J. Mol. Catal. A 145 (1999) 169.